DEPARTMENT OF PHYSICS, UNIVERSITY OF JYVÄSKYLÄ
RESEARCH REPORT No. 1/1986

LATE RADIATION DAMAGE IN BONE, BONE MARROW AND BRAIN VASCULATURE, WITH PARTICULAR EMPHASIS UPON FRACTIONATION MODELS

BY
MAUNU PITKÄNEN

Academic Dissertation
for the Degree of
Doctor of Philosophy

Jyväskylä, Finland
April 1986

URN:ISBN:978-951-39-9690-1
ISBN 978-951-39-9690-1 (PDF)
ISSN 0075-465X

Jyväskylän yliopisto, 2023

ISBN 951-679-495-5
ISSN 0075-465X

DEPARTMENT OF PHYSICS, UNIVERSITY OF JYVÄSKYLÄ
RESEARCH REPORT No. 1/1986

LATE RADIATION DAMAGE IN BONE, BONE MARROW AND BRAIN VASCULATURE, WITH PARTICULAR EMPHASIS UPON FRACTIONATION MODELS

BY
MAUNU PITKÄNEN

Academic Dissertation
for the Degree of
Doctor of Philosophy

To be presented, by permission of the
Faculty of Mathematics and Natural Sciences
of the University of Jyväskylä,
for public examination in Auditorium S-212 of the
University on April 26, 1986, at 12 o'clock noon.

Jyväskylä, Finland
April 1986

Preface

This work has been carried out during the years 1979-1984 at the Research Institute, University of Oxford, England and at the University Central Hospital of Kuopio and Tampere. I wish to express my thanks to these institutes for the excellent working conditions provided for me.

It is a pleasure for me to express my sincere gratitude to Dr. J.W. Hopewell, who guided me into this field of research. I warmly thank my teacher, Professor A. Rekonen for his ideas and encouragement during the course of this study. I am indebted to Professor E. Spring for his careful and critical reading of the manuscript.

To my co-workers, Docent T. Lahtinen Ph.D., Dr. T. Hietanen Dr.Med. and Docent A. Ojala M.D., I offer sincere thanks for enjoyable co-operation.

I am also indebted to Mr. J.D. Hopkins B.A. for revising the language of the manuscript.

To my wife and children I owe a great depth of gratitude for their patience and understanding.

This work was financially supported by grants from University of Oxford (Florey Studentship), from the Cancer Society of Pirkanmaa and from Emil Aaltonen Foundation.

Jyväskylä, April 1986

Maunu A. Pitkänen

ABSTRACT

X-ray induced changes in rat and human bone and bone marrow vasculature and in rat brain vasculature were measured as a function of time after irradiation and absorbed dose. The absorbed dose in the organ varied from 5 to 25 Gy for single dose irradiations and from 19 to 58 Gy for fractionated irradiations. The number of fractions varied from 3 to 10 for the rat experiments and from 12 to 25 for the human studies. Blood flow changes were measured using an ^{125}I antipyrine or $^{86}RbCl$ extraction technique. The red blood cell (RBC) volume was examined by ^{51}Cr labelled red cells. Furthermore, different fractionation models have been compared.

Radiation induced reduction of bone and bone marrow blood flow were both time and dose dependent (8,10,11). Reduced blood flow 3 months after irradiation would seem to be an important factor in the subsequent atrophy of bones (8). With a single dose of 10 Gy the bone marrow blood flow, although initially reduced returned to the control level by 7 months after irradiation (10).

In the irradiated bone the RBC volume was about same as that in the control side but in bone marrow the reduction was from 32 to 59 % (9,10).

The dose levels predicted by the nominal standard dose (NSD) formula produced approximately the same damage to the rat femur

seven months after irradiation when the extraction of ^{86}Rb chloride and the dry weight were concerned as the end points (9). However, the results suggest that the NSD formula underestimates the late radiation damage in bone marrow when a small number of large fractions are used (10). The present data for late changes in bone marrow do not permit an accurate assessment of the α/β ratio (probability of the component of irreparable events to the component of cumulative sublethal damage), but the results would suggest a value of between 2 and 4 Gy (10).

In the irradiated brains of the rats the blood flow was on average 20.4 % higher compared to that in the control group. There was no significant difference in brain blood flow between different fractionation schemes (12). The value of 0.42 for the exponent of N corresponds to the average value for central nervous system (CNS) tolerance that is available in the literature. The model used may be sufficiently accurate for clinical work provided the treatment schemes used do not depart too radically from standard practice.

CONTENTS

1.0 INTRODUCTION

The aim of radiotherapy is to destroy all or nearly all tumor cells without any lasting unacceptable damage to the normal tissue. Therefore, the radiation dose given to the treatment volume is quite often limited by the normal tissue tolerance.

According to time, the radiation induced normal tissue injury has been divided into three different phases

- Early changes which occur within hours after exposure are mainly related to changes in vascular volume and in the permeability of the cells. Cell death plays a minor role.

- Intermediate changes develop, depending on the tissue and cell type involved, ranging from a few days (intestine) to a few weeks (bone marrow, skin) or months (endothelial cells) after exposure and are principally caused by a disturbance of cell renewal although vascular changes are often also present.

- Late changes occur months or even years after irradiation and are characterized by vascular lesions and fibroplastic changes. There may be intercellular fibrosis, replacement of parenchymal cells by fibrous tissue, fibrotic thickening of the walls of small arteries and arterioles and deposition of collagen in capillary lumina. There is more variability in the latent intervals between irradiation and clinical

manifestation of late injury: 6-24 months or longer for myelitis, 6 months to many years for progressive fibrosis in connective tissue (1).

The normal tissue tolerance can not be defined unambiguously. It is dependent, among other things, on the following factors:

- The dose per fraction (i.e. the number of fractions), which is determined mainly by the effect of repair processes in the irradiated tissue. The factor has been taken into the consideration in different fractionation models (2) (chapter 3.0).

- The overall treatment time. After a certain repairing time, the time factor is affected mainly by the cellular repopulation rate of the tissue in question. Acutely-reacting tissues (with high repopulation rates) do have a significant time factor. However, for late reactions the effect of overall time appears to be small or absent. The effect of time has been predicted by different models in chapter 3.0.

- Dose rate. There are mainly two different processes involved in the dose rate effect: 1.) the repair of sublethal radiation damage taking place during the irradiation, 2.) repopulation occurring as a result of cell division during a protracted exposure. The dose rate effects have been predicted by different models (3,4,5,6).

- The tissue and cell type involved. The type of primary target cells is dependent on the absorbed dose. With the dose levels used in clinical radiotherapy the target cells are the parenchymal cells and/or the vascular endothelial cells.

- The volume of tissue irradiated. The cell lethality is not a function of field size, but the tissue tolerance is affected by this factor. The volume effect may be due to the migration of unaffected stem cells from surrounding tissues. The effect has been described by the factor Z^y, where Z is the field diameter and y a fractional exponent for the normal tissue in question (7).

- The quality of the radiation. The factor is associated with a linear energy transfer of secondary charged particles and also with a relative biological effectiveness of the beam.

In the present study, radiation induced vascular changes in bone, bone marrow and brain tissue were measured as a function of time and absorbed dose. Furthermore, the effects of fractionated X-ray doses on the vasculature have been studied and compared to different fractionation models.

This thesis is based on the following publications:

(8) Pitkänen M.A. and Hopewell J.W.: Functional changes in the vasculature of the irradiated rat femur, their implications for late effects. Acta Radiol. Oncol. 22:253-256,1983

(9) Pitkänen M.A. and Hietanen T.: Late radiation damage to the rat femur and the NSD formula. Strahlentherapie 160:394-397, 1984

(10) Pitkänen M.A. and Hopewell J.W.: Effects of local single and fractionated X-ray doses on rat bone marrow blood flow and red blood cell volume. Strahlentherapie 161:719-723,1985

(11) Lahtinen T., Pitkänen M.A. and Ojala A.: Effects of fractionated radiotherapy on bone blood flow in man. Strahlentherapie 162:37-40,1986

(12) Pitkänen M.A. and Hopewell J.W.: Response of rat brain tissue for the extraction of ^{125}I antipyrine after single and fractionated X-ray doses. A comparison of fractionation models applied to CNS. Acta Radiol. Oncol. 24:445-450,1985

2.0 PURPOSE OF THE PRESENT STUDY

(1) to evaluate characteristics of different fractionation models;

(2) to study error sources in the determination of absorbed dose in bone, bone marrow and brain tissue;

(3) to study late radiation induced vascular changes in bone, bone marrow and brain tissue;

(4) to study the role of vascular damage in the development of late radiation induced changes in tissue with the dose levels used in clinical radiotherapy;

(5) to compare the effects of single and fractionated X-ray doses on the vasculature;

(6) to test the fractionation models using vascular changes as the end point;

(7) to investigate the need for different parameters for different tissues in fractionation models.

3.0 DOSE RESPONSE MODELS

3.1 Nominal standard dose (NSD) formula

The isoeffect lines introduced by Strandqvist (13) describe the total dose required to produce the observed effect as a function of the overall treatment time or of the fraction size. Ellis (14) observed that the isoeffect curves for skin reactions relating the total dose (tolerance dose, D_{tol}) to the overall treatment time give a roughly linear relationship on a log-log plot. The slope of this isoeffect line was 0.33. The exponent of time was then divided into two separate parts: the number of fractions, and the overall treatment time (14). The difference of the slopes between the tumor effect and the normal skin effect was 0.11. He explained the difference as the participation of homeostatic control in the skin effect,which was therefore related to the time factor.

$$D_{tol} = NSD \cdot N^{0.24} \cdot T^{0.11} \qquad (3.1)$$

where N = number of fractions necessary to bring skin to tolerance by this protocol, T = over-all treatment time in days and NSD = nominal standard dose, a constant for a given volume of normal tissue irradiated. The dimension of the NSD is called ret (radiation equivalent therapy). The NSD formula was derived from early skin reactions. The most important point in the NSD formula was that the first time, the time factor and the number of

fractions (the dose per fraction) were taken into consideration separately.

Based on the NSD formula, Kirk et al.(15) have also developed the cumulative radiation effect (CRE) concept for sub-tolerance levels of radiation doses, as the original concept of NSD pertain only to full tolerance of the skin:

$$CRE = d \cdot n^{0.76} \cdot t^{-0.11} \qquad (3.2.)$$

where d = dose per fraction, n = the number of fractions under a certain protocol ($n \leqq N$) and n treatments given in an overall period of t days ($t \leqq T$). The dimension of CRE is called reu (radiation effect unit).

To simplify the practical use of the NSD concept Orton and Ellis (16) have introduced the concept of partial tolerance (PT):

$$PT = NSD \cdot \frac{n}{N} \qquad (3.3.)$$

Further, they have defined the "time,dose and fractionation factor" (TDF):

$$TDF = n \cdot d^{1.538} \cdot \left(\frac{T}{N} \right)^{-0.169} \cdot 10^{-3} \qquad (3.4.)$$

The PT and TDF formulas were introduced to apply the NSD concept to situations in which the end point of the radiation effect is not on the level of normal tissue tolerance. As PT, TDF is additive and the TDF value for the total treatment is given by:

$$TDF = \sum_i TDF_i \qquad (3.5.)$$

where i = one treatment course.

A decay factor (DF) for a rest period of duration R days following a partial course of treatments of T days, has been given by Winston et al.(17):

$$DF = \left(\frac{T}{T+R} \right)^{0.11} \qquad (3.6.)$$

The exponent of 0.11 is the same as that for time in the NSD concept.

The dimension of the NSD formula is arbitrary. To get the right dimension, the time, T, should be divided by T_0 (T_0 = 1 day). Thus the formula obtain the form:

$$D_{tol} = NSD \cdot N^{0.24} \cdot \left(\frac{T}{T_0} \right)^{0.11} \qquad (3.7.)$$

The same modification can also be made for the CRE and the TDF formulas.

Since Ellis (14) published his formula concerning the influence of the fraction number and time on the reaction of the skin to radiation treatment, the formula has been applied to most normal tissues by the same values of parameters. However, many clinical situations have shown that large doses per fraction can cause severe late damage if the total dose was calculated by the NSD formula (18,19,20,21,22,23,24,25,26,27,28,29,30,31,32). The NSD concept is satisfactory in application only to early reactions (33) and to the skin. Therefore, modified forms of Ellis' concept have been developed. The exponents of N and T have been examined for late reactions in different tissues. Cohen and Creditor (34,35) collected the data from literature with radiation

injuries in the brain, kidney,lung and intestine. The exponents of N and T used in all the modified Ellis' formulas for CNS tolerance that are available in the literature are presented in Table I.

3.2 Composite multi-target (CMT) model

In target theory the cells contain a number of sensitive sites or targets (43,44,45). If any one of these targets remains intact the cell will not be sterilised. One or more energetic events or hits is required to inactivate the target.

In the single hit-single target model only one hit is needed to kill the cell, which contains only one target. The resulting equation for the surviving fraction (S_J) is a simple exponential function:

$$S_j = e^{-J \cdot D} \qquad (3.8.)$$

where D = the absorbed dose, and J = a parameter with the dimension 1/Gy, which may be thought of as the average number of hits produced per Gy in a volume of the same size as the target. The constant of proportionality J may be expressed by $1/D_0$, as well. Thus the dose D_0, the mean lethal dose, is the dose required to reduce the population of cells to 37 % of its initial value.

In the single hit-multi target model the cell contains a number of targets (n_t) and one hit is needed for each target to inactivate the cell. The survival fraction (S_K) can be presented by the formula:

$$S_k = 1 - (1 - e^{-K \cdot D})^{n_t} \qquad (3.9.)$$

Bender and Cooch (44) have found that the cell survival curve consists both of single hit-single target events and of single hit-multi target events. The total survival (S) is the product of the individual survival of inactivating by both mechanisms:

$$S = S_j \cdot S_k = e^{-J \cdot D}(1 - (1 - e^{-K \cdot D})^{n_t}) \qquad (3.10.)$$

So it is supposed that the killing effect of the two radiation components are independent of each other. The model assumes that the cell consists of an irreversible single event component and of a multitarget component having an Elkind - type early recovery capacity. Therefore, K is the radiosensitivity constant for cumulative sublethal effects (multitarget components) and J is a measure of the initial slope of the survival curve (single target components).

For fractionated treatment the survival after N equal treatments is:

$$S_N = \{ e^{-J\ D} (1 - (1 - e^{-K\ D})^{n_t}) \}^N \qquad (3.11.)$$

The equation is called the composite multitarget model (46,47). Using the CMT model Cohen and Creditor (34,35,48) have evaluated the available information in literature on radiation injury to a

specific organ or tissue. They have analyzed the parameters of J,K and n_t for the brain,kidney, lung, skin and intestine. The isoeffect tables for the above mentioned tissues are presented, as well. The survival curves for the brain (n_t=19, J=0.09, K=0.74) and the skin (n_t=17, J=0.34, K=0.59) are presented in Fig. 3.1., the number of fractions (N=1, 30) being as a parameter.

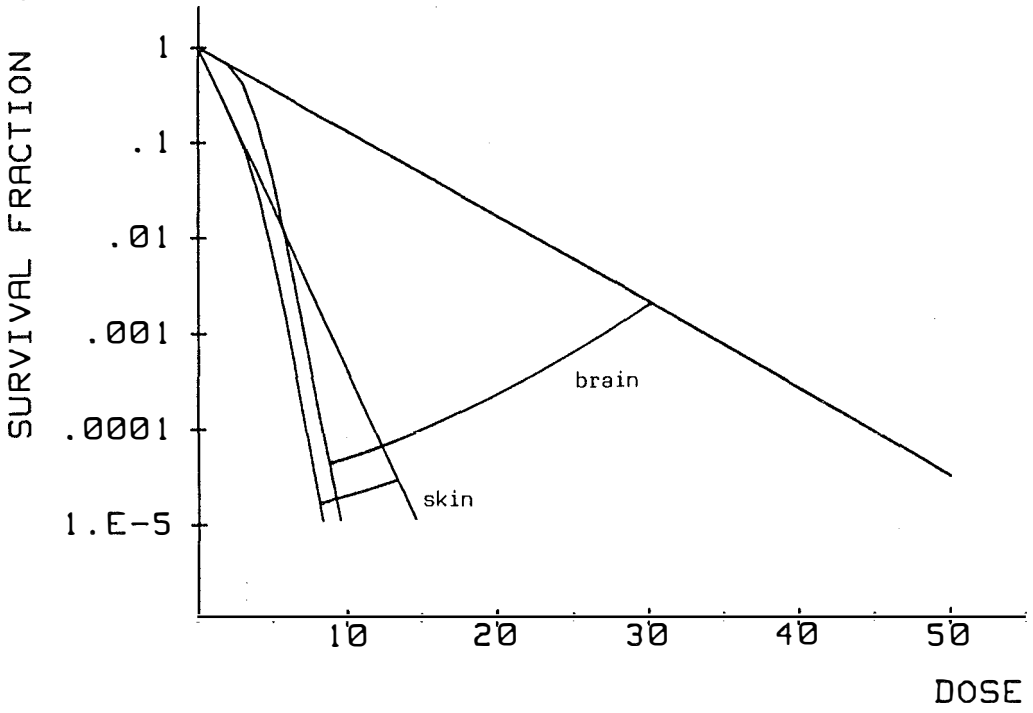

Fig. 3.1. The survival curves according to the composite multitarget model for skin (n_t=17,J=0.34,K=0.59) and for brain (n_t=19,J=0.09,K=0.74), the number of fractions (N=1 or 30) being as a parameter.

The so-called "two component model" of Wideröe (49,50) has in principle the same mathematical contents as that of the CMT model.

Spring and Paasikallio (51) have modified the single-hit multi-target model. Based on clinical studies reported in literature a value is given for each parameter. The formula is multiplied by the exponential regeneration term exp(LT). Because hypoxic cells dominate towards the end of the radiotherapy course, a correction term is subtracted from the equation. The survival equation thus becomes:

$$S_N = (1 - (1 - e^{d/300})^{1.5}) \cdot e^{0.1 \cdot T} - 0.01 \cdot e^{-N} \qquad (3.12.)$$

3.3 Linear quadratic (LQ) model

The linear quadratic model is a two parameter exponential survival probability function (S) with a quadratic component (52):

$$S = e^{-(\alpha \cdot d + \beta \cdot d^2)} \qquad (3.13.)$$

where α describes the probability of irreparable or single hit events, which determine the initial slope of the survival curve (analogous to J in the CMT model)and β is involved in the cumulative sublethal component (analogous to K in CMT model). For fractionated treatments the survival after N equal doses is:

$$S_N = \{ e^{-(\alpha \cdot d + \beta \cdot d^2)} \}^N \qquad (3.14.)$$

In logarithmic form the equation is:

$$\ln S_N = N \cdot (\alpha \cdot d + \beta \cdot d^2) = N \cdot d \cdot (\alpha + \beta \cdot d)$$

If the total dose (D_t) is equal to Nxd, so:

$$\frac{\ln S_N}{D_t} = \alpha + \beta \cdot d$$

Therefore in a linear plot of $\ln S_N / D_t$ against single dose (d) gives α as an intercept of the ordinate.

The LQ model has been applied to the number of normal tissues (6,40,53,54,55) both for acute and late effects. The ratio of linear to quadratic term (α/β) is around 10 Gy for acute and about from 2 to 4 Gy for late effects. Barendsen (6) derived the parameters α and β from the data of Liversage (3) for mouse bone marrow, using the LD(50/20day) end point. A ratio of α/β of 4.0 Gy was obtained for these early reactions in bone marrow after whole body irradiation. The parameters are not found for bone tissue. The data available in the literature regarding the ratio of α/β for the central nervous system tolerance is presented in Table II.

Author	Site	Exponent of	
		N	T
Wara et coll. 1975	human thoracic cord	0.38	0.06
van der Kogel 1977	rat spinal cord		
	- cervical	0.44	0.05
	- lumbar	0.42	0.05
Masuda et coll. 1977	rat thoracic spinal cord		
	- paralysis in 50%	0.44	0
	- 5% risk of paralysis	0.36	0
White and Hornsey 1978	rat lumbar spinal cord	0.40	0.07
Hornsey et coll. 1981	rat brain	0.38	0.02
Pezner and Archambeau 1981	human brain and optic nerves	0.45	0.03
Wigg et coll. 1981	human brain		
	- large volume	0.46	0.09
	- small volume	0.41	0.04
	human spinal cord (myelitis in 50%)	0.43	0
	human optic nerve and chiasm	0.33	0
	mean value for whole CNS in humans	0.40	0
Cohen and Creditor 1981	human spinal cord	0.42	0.06
Cohen and Creditor 1983	human brain	0.56	0.03
	mean	0.42	0.05
	sd	0.05	0.02

Table 1. Modified Ellis' formulas applied to the central nervous system

Author	Site and end point	α/β
van der Kogel 1982	rat spinal cord	
	- cervical white matter necrosis	2.0
	- cervical vascular damage	2.8
	- lumbar myelopathy	3.9
Cohen and Creditor 1981	human spinal cord	
	- myelopathy	2.5
Barendsen 1982	rat spinal cord	
(from Hornsey and White 1980)	- lumbar myelopathy	4.5
Barendsen 1982	rat brain	
(from Hornsey et coll. 1981)	- LD 50/1y	6.0
Cohen and Creditor 1983	human brain	
	- 5% risk of necrosis	4.2
Fowler 1983	rat spinal cord	
(from Leith et coll. 1981)	- lumbar myelopathy	3.9
Fowler 1983	rat spinal cord	
(from White and Hornsey 1978)	- cervical myelopathy	1.8

Table 2. The ratio of linear to quadratic terms (α/β) in the LQ model

3.4 Repair-Misrepair (RMR) model

The RMR model (58) supposes that the cellular effects of ionizing radiation have four different phases:

1. The initial physical energy transfer and redistribution of energy by physical events.
2. Migration of the deposited energy and the establishment of long-lived molecular lesions as a result of radiation chemistry.
3. Biochemical processes including repair or enhancement, coupled with progression of cells through various physiological states.
4. Genetics and evolutionary processes.

The radiation chemical phase overlaps the time sequence of radiation physics. The time scale of radiation biochemistry can range from minutes to days. The repairing of genetic damage may continue through several generation of cells.

The RMR model regards the fate of the early radiation induced lesions in cells as uncertain. A probability factor is introduced to describe whether these lesions can be perfectly repaired or lead to lethality due to imperfect misrepair, which includes incomplete repair.

The model describes the yield of relevant macromolecular lesions per cell as a function of dose (D), the time-dependent (t) transformations of these lesions and the time and dose dependent probabilities for survival (S), lethality (L) and mutation (M). The parameter U stands for "uncommitted", which is what the lesions are before they are subject to enzymatic repair and

modification. The repair states (R) are defined as the result of transformations of U states following enzymatic repair. The model has two R states: R_1 is the yield of a linear repair process assumed to proceed as a monomolecular chemical reaction and R_q is the yield per cell of a repair process involving interaction between pairs of U lesions (quadratic repair process).

The time-dependent behaviour of U is described by the first order quadratic differential equation:

$$dU/dt = -c_1U(t) - c_qU^2(t) \qquad (3.15.)$$

where c_1 and c_q are the coefficients of linear and quadratic repair, respectively. Integrating from time 0 to t:

$$U(0) - U(t) = \int_0^t c_1U(t)dt + \int_0^t c_qU^2(t)dt$$

With the definitions:

$$R_1 = \int_0^t c_1U(t)dt \quad , \quad R_q = \int_0^t c_qU^2(t)dt$$

we have:

$$U(t) + R_1(t) + R_q(t) = U(0) \qquad (3.16.)$$

For a specific cell type in a specific state, c_1 and c_q are constant and independent of time and dose. Let $U(0)=U_0$, $R_1(0)=R_q(0)=0$, $U(\infty)=0$ and $R_r=c_1/c_q=$ the repair ratio, and a simple solution exists for U, R_1 and R_q.

If the cell repairs the damage accurately, making the DNA sequencing exactly like it was before radiation damage occurred, the repair is called "eurepair". The other types of repair are

variations of misrepair, ranging from viable mutants to alterations that eventually cause cell death. There are six different applications of the RMR model. These cases are chosen to interpret a variety of types of radiobiological experiments. The simplest RMR model supposes that all quadratic repair results in lethal misrepair. According to Poisson statistics this leads to the survival equation:

$$S(t) = e^{\{-R_q - U)} = e^{-aD} \{ 1 + aD/R_r \}^{R_r} \qquad (3.17.)$$

where a is the yield of U lesions per rad and R_r is the repair ratio. The other five cases can be derived analogously.

4.0 DETERMINATION OF ABSORBED DOSE FROM THE EXPOSURE

4.1 Absorbed dose in air

The quantity of exposure is defined in ICRU Rep. 33 (59):

The exposure, X, is the quotient of dQ by dm where the value of dQ is the absolute value of the total charge of ions of one sign produced in air when all the electrons (negatrons and positrons) liberated by photons in air of mass dm are completely stopped in air, X=dQ/dm (C/kg).

If the mean energy required to produce an ion pair in air is W_{air}, the energy imparted to the air by the electrons released from the mass dm is therefore according to the definition of exposure:

$$\frac{dQ}{e} W_{air} = \frac{X\ dm}{e} W_{air}$$

where e is a charge of an electron.

The energy imparted per unit mass of air, i.e. the absorbed dose in air (D_{air}) is:

$$D_{air} = X \frac{W_{air}}{e} \qquad (4.1.)$$

The formula is valid only under conditions of electronic equilibrium.

4.2 Absorbed dose in other materials

The energy absorbed per unit mass of various materials subjected to the same energy fluence will be proportional to the mass energy absorption coefficient, μ_{en}/ρ, of those materials. Therefore, the absorbed dose, D_{ma}, in some other material (ma) is given by:

$$D_{ma} = X \frac{W_{air}}{e} \frac{(\mu_{en}/\rho)_{ma}}{(\mu_{en}/\rho)_{air}} \qquad (4.2.)$$

The coefficient of absorption (f) is defined from the equation (4.2):

$$f = \frac{W_{air}}{e} \frac{(\mu_{en}/\rho)_{ma}}{(\mu_{en}/\rho)_{air}} \qquad (4.3.)$$

The absorbed dose can be defined in terms of air kerma instead of exposure. Air kerma is the energy equivalent of the air ionisation in the definition of exposure with a correction for bremsstrahlung production. The energy per unit mass equivalent of exposure X is $X\ W_{air}/e$ and the allowance for bremsstrahlung production is made by using the ratio of the mass energy transfer (tr) and mass energy absorption (en) coefficients for air:

$$K_{air} = X \frac{W_{air}}{e} \frac{(\mu_{tr}/\rho)_{air}}{(\mu_{en}/\rho)_{air}} \qquad (4.4.)$$

From equation (4.2) we obtain:

$$D_{ma} = K_{air} \frac{(\mu_{en}/\rho)_{ma}}{(\mu_{tr}/\rho)_{air}} \qquad (4.5.)$$

Also $\mu_{en}/\rho = (\mu_{tr}/\rho)(1-g)$, where g is the fraction of the energy of secondary charged particles that is lost to bremstrahlung in the material.

4.3 Determination of absorbed dose and exposure from cavity theory

4.3.1 Bragg-Gray cavity theory

In the Bragg-Gray cavity theory (60,61) it is considered a medium uniformly irradiated by photons and of sufficient dimensions that electronic equilibrium is established at a place within it in which a small gas (usually air) filled cavity is introduced. The cavity is so small that it does not change the number, energy or direction of the electrons crossing the cavity surface, providing that scattering of electrons in the cavity can be neglected. The ratio of the electron energy lost per unit mass in the two materials will be the same as the ratio, s_{maga}, of the mass stopping powers, $(S/\rho)_{ma}/(S/\rho)_{ga}$, of the medium and the gas for the electrons concerned. Therefore, the absorbed dose, D_{ma}, in the medium is given by:

$$D_{ma} = s_{maga} \times \frac{W_{ga}}{e} = s_{maga} D_{ga} \qquad (4.6.)$$

which is the Bragg-Gray formula.

The cavity theory assumes:

(1) that charged particle equilibrium exists in the absence of the cavity;

(2) -that the cavity does not disturb the charged particle fluence or its distribution in energy and direction;
-that charged particle production in the cavity is negligible or no different from that in an equal mass of surrounding medium;

(3) that the mass stopping power ratio, s_{maga}, does not vary with energy;

(4) that the secondary charged particles lose energy through a process of continuous slowing down.

When the cavity is very small and photon interactions within it are negligible, the ratio of the energies absorbed per unit mass of the medium and of the gas is the same as the stopping power ratio for electrons in the two materials. The stopping power ratio is almost independent of the energy of the electrons and in fact assumed to be constant. As the cavity increases in size photon interactions in it will become significant and when the radius of the cavity exceeds the maximum range of electrons coming from the surrounding medium, the absorbed dose at the centre of the cavity will be determined by these photon interactions and will be proportional to the mass energy absorption coefficient of the cavity material. Thus as the size of the cavity increases the ratio of the absorbed doses in the medium and cavity gradually changes from s_{maga} to $(\mu_{en}/\rho)_{ma}/(\mu_{en}/\rho)_{ga}$.

4.3.2 Spencer-Attix and Burlin cavity theories

If there are large discrete energy losses, resulting in delta-ray production (interactions of fast secondary electrons), some of the energy will be carried out of the volume. Spencer and Attix (62) derived an approximate formula for the restricted stopping power ratio (for very small cavity dimensions) which takes into account the production of fast secondary electrons and is based on an analysis of the different electron contributions of the medium (ma) and the cavity (ca):

$$f_{cama} = (Z/A)_{cama}\{1+\frac{1}{E_o}(\int_{\Delta}^{E_o} R_{ma}(E_o,E)(\frac{B_{ca}(E)}{B_{ma}(E)}-1)dE + \Delta R_{ma}(E_o,\Delta)(\frac{B_{ca}(\Delta)}{B_{ma}(\Delta)}-1))\} \qquad (4.7.)$$

where

$R_{ma}(E_0,E) = I_{ma}(E_0,E)\ S_{ma}(E)$

$I_{ma}(E_0,E)$ is the equilibrium electron energy spectrum in the medium generated by primary electrons with energy E_0

Z and A are the effective atomic number and atomic weight, respectively

B is the stopping number equal to S/(Z/A)

Δ was defined rather arbitrarily as the electron energy whose range is equal to the cavity thickness. The equation (4.7.) neglects the effects of cavity geometry and a cavity source term

arising from gamma-ray interactions in the cavity. Delta is restricted to energies greater than the K binding energy of electrons and E_0 to energies for which the bremsstrahlung contribution is not significant.

The general cavity theory (63) is applied to the intermediate size of the cavity, whose dimensions are comparable with the electron range, and in consequence with that the electron spectrum within the cavity is neither completely determined by the medium nor the cavity material. The theory gives the restricted stopping power ratio in the following form:

$$f_{cama} = (Z/A)_{cama}\{1+\frac{d_w}{E_o}(\int_{\Delta}^{E_o} R_{ma}(E_o,E)(\frac{B_{ca}(E)}{B_{ma}(E)}-1)dE + \Delta R_{ma}(E_o,\Delta)(\frac{B_{ca}(\Delta)}{B_{ma}(\Delta)}-1))+(1-d_w)((Z/A)_{maca}(\mu_{en}/\rho)^{-1}_{cama})\} \quad (4.8.)$$

or in more simple form:

$$f_{cama} = d_w \bar{s}_{cama} + (1-d_w)(\bar{\mu}_{en}/\rho)_{cama} \quad (4.9.)$$

where the first term represents electrons generated in the medium and the second term is an additional term representing electrons generated in the cavity via photon interactions. The factor d_w is a weighting factor which expresses the reduction of the electron fluence from the medium inside the cavity. Let g_p be the average path length of electrons crossing the cavity. On average, the medium spectrum will be reduced by the factor:

$$d_w = \int_0^{g_p} e^{-(\beta_e x)}dx \;/\; \int_0^{g_p} dx = \frac{1-e^{-(\beta_e g_p)}}{\beta_e g_p} \quad (4.10.)$$

where β_e is the effective mass attenuation coefficient of the electron flux penetrating the cavity material.

Horowitz and Dubi (64) have introduced a new weighting factor d'_w expressing the average path length for medium and cavity generated electrons as unequal. Thus :

$$d'_w = \int_0^{g'_p} (1 - \exp(-\beta_e x))\, dx / \int_0^{g'_p} dx \qquad (4.11.)$$

where g'_p is the average path length for electrons created by photon fluence interactions within the cavity. However, this modification is not accepted in general (65,66).

4.4 The structure of bone from the dosimetric point of view.

The structure of the bones varies in the different parts of the body (e.g. long, short and "flat" bones). But only the femur, a typical long bone, is an object for dosimetric investigation in this work. The major part of the long bone is shaft (diaphysis), which is like a hollow tube of hard bone (cortex) containing yellow marrow. The cortex is covered on the outside with a layer of fibrous tissue (the periosteum) and lined on the inside with cells of the endosteum. Each end of the bone shaft is filled with fine lamellae of bone, which in the numerous cavities contain the red marrow. The network of bone lamellae is called trabecular bone. The end of the bone is called the epiphysis and the trabecular part below the epiphyseal plate is called the metaphysis, a region where bone growth takes place.

Cortical bone is a mineralized matrix in which cells and organized soft tissue structures live and function.

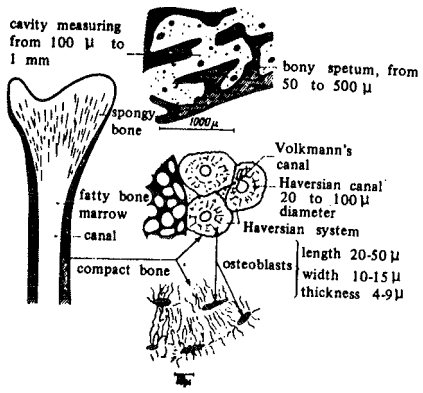

Fig. 4.1. The structure of bone (67).

The structure of the cortex is organized in units called Haversian systems (osteons). Each osteon has a central canal (the Haversian canal) through which run nutrient blood vessels. The matrix contains numerous small cavities (the lacunae) in which osteocytes line and are nurtured by means of very small canals (canaliculi) that connect them to each other and to the central canal. The osteocytes and the cells and contents of the Haversian canals constitute the soft tissue component of cortical bone and represent the radiosensitive part of the cortical bone structure. The diameter of the Haversian canal is approximately from 20 to 100 µm, the typical diameter being 50 µm. The diameter of the lacunae is around 5 µm and the diameter of the canaliculi is under 1 µm (67).

The trabecular network consists of interconnecting cavities. The lamellae have dimensions of the order of 100 µm in thickness and do not incorporate blood vessels as in Haversian systems. The

cavities have a linear dimension which varies from 50 μm or less, as much as 2000 μm, typically from 200 to 500 μm.

The high density of the bone matrix is contributed by the crystals of the calcium salt hydroxyapatite, $Ca_{10}(PO_4)_6(OH)_2$, seeded along and between the collagen fibrils. Bone substance contains a large quantity of elements with relatively high atomic numbers, mainly phosphorous and calcium. The presence of salts in bone determines its mean atomic number, typically 13.8. Depending on the content and the size of bone cavities, the density of cortical bone varies about from 1100 to 1900 kg/m^3.

4.5 Determination of absorbed dose in bone.

The coefficient of absorption (f) for determination of the absorbed dose has been measured for compact bone as well as for soft tissue as a function of photon energy. The f value for compact bone (f_{boga}) gives the energy absorption in the calcified matrix, which constitutes the mineralized component of the bone structure. In compact bone (ρ =1800 kg/m^3)the f_{boga} value for ^{60}Co radiation is 0.92 (in muscle (f_{muga}) 0.96), and for 250 kV X-rays (HVL of 2.0 mmCu)the f_{boga} value is 1.32 and f_{muga} is 0.95 (67). Therefore, the absorbed dose in bone with ^{60}Co rays is only a little less than that in muscle (dose in bone/dose in muscle=0.96). Using 250 kV x-rays the absorbed dose in bone is about 1.4 times higher than that in muscle.

The absorbed dose in the calcified matrix of bone can be calculated according to the equation (4.2.):

$$D_{bo} = X \frac{W_{air}}{e} \frac{(\mu_{en}/\rho)_{bo}}{(\mu_{en}/\rho)_{air}} \qquad (4.12.)$$

If the dimensions of the cavity in bone are much smaller than the maximal pass of the secondary electrons, their flux is homogeneous in the soft tissue contained in the cavity. However, since the electrons lose energy at different rates in compact bone and in soft tissue, the previous equation must be multiplied by the ratio of the mass stopping power of tissue to the calcified matrix to get the absorbed dose in the cavity:

$$D_{\text{soft tissue in bone cavity}} = (s)^{\text{soft tissue}}_{\text{bone}} D_{bo} \qquad (4.13.)$$

Calculating from the data (68) we obtain for ^{60}Co irradiation: $^{water}s_{bone} = 1.08$ and about the same value for 100 kV photons. Therefore, $D_{\text{soft tissue in bone cavity}} = 1.1 \times D_{bone}$.

The secondary electrons arising during ^{60}Co irradiation have a relatively long path length, around 5000 µm in water, and the flux of the secondary electrons in soft tissue and in compact bone substance is almost identical (ICRU 33 (59):The particle flux, N, is the quotient of dN by dt, where dN is the increment of particle numbers in the time interval dt, N=dN/dt). Therefore in the case of ^{60}Co irradiation the cavity size can be assumed as being small compared to the electron range.

With 250 kV X-rays (HVL of 2.0 mmCu), the determination of the

dose distribution is a more complicated task. The range of photo electrons in soft tissue and in compact bone is 90 um and 57 µm, respectively (69). Therefore, the charged particle equilibrium is disturbed in most of the cavities.

The changes in ionization for different cavity sizes (the space between parallel bone plates) have been studied by Spiers (69). The changes are dependent both on the energy of the radiation and the cavity size. With about 250 kV X-rays, in the middle of the cavity the ratios of the ionisation of soft tissue in bone cavity/ in "native " soft tissue for the cavity sizes of 1, 10, 50 and 100 µm are 2.3, 2.1, 1.7 and 1.2, respectively.

5.0 LATE RADIATION INDUCED VASCULAR DAMAGE AND ITS IMPORTANCE FOR LATE EFFECTS IN NORMAL TISSUE

The response of tissue to irradiation will depend on the turnover times and radiosensitivities of both parenchymal and vascular components and on any interactions between the various types of cells. Furthermore, the target cells in the organ may depend on the radiation dose used (71). However, after therapeutic doses of irradiation, tissues which show no early reactions in parenchymal cells show progressive vascular changes over a period of several months (72,73,74). Furthermore, it has been shown that these

histological changes in blood vessels precede the atrophy of parenchymal cells (71,72,75,76).

A number of different techniques have been used to measure the radiation induced vascular damage: structural changes in the blood vessel walls, blood flow, blood volume, vascular permeability, endothelial cell survival and cell proliferation in the blood vessel wall. Vascular damage may be arbitrarily divided into early, intermediate and late changes, with respect to the time of lesion after irradiation. The earliest effect of radiation on blood vessels is erythema, which is due to the dilatation of the capillaries. Depending on the dose level it develops within a few hours or after a few days. In intermediate changes, observed at 2-6 months, irregularly spaced constrictions appear, particularly in the walls of the arterioles (77,78). The changes are characterized by the swelling of endothelial cell cytoplasm and the sloughing of endothelial cells (79). Late changes, observed at 6 months or later, are characterized by degenerative changes in the arteries, arterioles and capillaries. Late changes include endothelial proliferation to the point of obliterating capillaries (80), the thickening of the basement membrane and replacement of the capillary lumen by collagen (81). Furthermore, teleangiectatic vessels are seen in some irradiated tissues (82). Arteries with regions of dilatation and constriction are often found, as well (78).

The functional changes in irradiated tissues have been studied by blood flow, blood volume and vascular permeability measurements. In the estimation of blood flow the wash-out and extraction

techniques are the most frequently used. The wash-out methods are based on the use of freely - diffusible tracers. In the extraction techniques the tracer is given intravenously or by intra cardiac injection. The initial distribution within an organ or tissue will depend on what proportion of the cardiac output supplies it. Potassium-42, rubidium-42 and iodo-antipyrine (^{125}I) are usually used as the tracer (83). Blood volume changes are measured with ^{51}Cr labelled red blood cells. The permeability of the vessels have been studied using two different tracers. The tracer under study is compared to the reference tracer, which can stay in the vascular space until the time of measurement. The reference tracer may be the red blood cells or some proteins labelled with radioisotopes (84,85). The origin of the increased vascular permeability observed during acute radiodermatitis is unknown, but suggests direct vascular injury. There is one hypothesis, which explains the development of fibrosis in irradiated tissue by increased permeability. In this hypothesis the primary radiation lesion, due to an increased vascular permeability, leads to edema and the deposition of fibrin in the interstitial space and blood vessel walls. The fibrin is subsequently replaced by collagen fibers (86). The increase in interstitial fibrosis may lead to parenchymal atrophy, which initiates a second phase of increased vascular permeability, again resulting in the deposition of collagen, this time in the place of parenchymal cells. An alternative hypothesis for the development of late fibrosis is that radiation alters the metabolism of collagen by the surviving cells.

Endothelial and smooth muscle cells are the main cellular

components of the walls of blood vessels. The cell survival characteristics of endothelial cells have been measured by counting vascular capillaries in vivo (87,88). Depending on the in vivo methods used D_0 values from 1.7 to 10.3 Gy have been obtained. Endothelial cells proliferate slowly in normal tissue. The labelling index in normal endothelium is usually less than 1 % (82). Very limited data is available regarding the effects of radiation on endothelial proliferation. Fajardo and Stewart (72) and Hirst et al. (89) have observed an increased endothelial proliferation after irradiation. However, the changes were transient and the proliferation returned to the control level within about 100 days. Hirst et al. (89) have studied the time and dose related changes in the relative numbers of endothelial and smooth muscle cell nuclei in the wall of arterioles in the irradiated mesentry in the mouse (Fig 5.1.(90)).

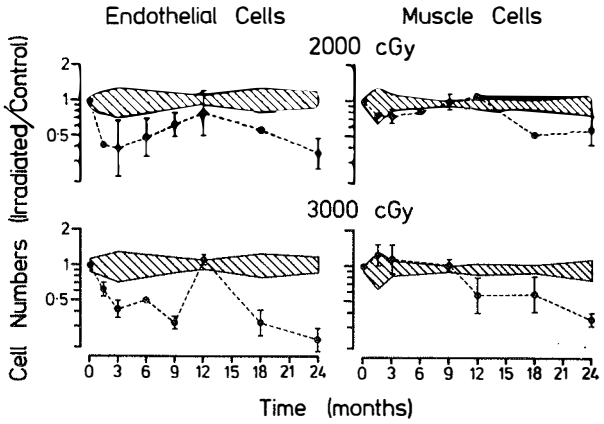

Fig. 5.1. Time related changes in the relative numbers of endothelial and smooth muscle cell nuclei in the wall of arterioles in the irradiated mesentry of the mouse (90).

With the lower dose level used the minimum numbers of endothelial cells were observed at 3 months. The endothelial cell population

returned to approximately the control level over 9-12 months. A reduction in the numbers of smooth muscle cells was seen after 12 months postirradiation. This loss of smooth muscle cells may be related to the thickening of the walls of the arterial and venous limbs of the circulation.

6.0 MATERIAL

Adult, Spraque-Dawley rats were used in this study as the animal model (8,9,10,12). From 5 to 10 rats were included in each dose group or in each fractionation scheme.

The study of the effects of the fractionated radiotherapy on bone blood flow in man (11) included 10 patients. The age of the patients was from 23 to 76 years, with the mean 57.4 years (15.9 1SD).

7.0 METHODS

The rats were irradiated with 250 kV X-rays (half value layer of 1.4-1.5 mm copper) under chloral hydrate anaesthesia (300 mg/kg body weight). The absorbed dose was determined by using an 0.6 cm^3 ionisation chamber. The dose rate varied from 1.27 to 2.17 mGy/s. The dose rate was verified by the National Standard Dosimetry Laboratory. In the rat studies the absorbed dose in the organ was determined according to the maximum depth dose. For blood flow and volume measurements the tracers were injected under chloral hydrate anaesthesia, as well. For bone irradiations the closure of the epiphyseal plates was checked roentgenologically.

In reference (8) the left femur of each animal was locally irradiated with a single dose of 5,10,15,20 and 25 Gy. At intervals of 1,3 and 7 months after irradiation the bone blood flow changes were measured using an ^{125}I antipyrine extraction technique (83), where a bolus of ^{125}I antipyrine was injected intravenously. After an interval of 15 seconds the animals were killed by decapitation. Both femurs were removed and all soft tissue was carefully removed. The activity of the whole femur was measured. The bones were then divided into 3 pieces at the levels of the epiphyseal plates and most of the marrow was removed by flushing with water. Any residual marrow was removed by shaking the bone pieces in a chloroform-ether solution. The activity of the bone fragments was calculated relative to unit mass of bone tissue. The bones were dried and the calcium and phosphorous

content was measured (91). The significance of difference between irradiated and control femurs (in the same animal) was estimated using a one-tailed t-test i.e. the ratio of irradiated/control was significantly lower than one.

In reference (9) the left femur of each animal was irradiated in 3,6 and 9 fractions (F) over 3 weeks. The dose levels used were based on the NSD value of 1450 and 1900 ret on the basis of the single dose irradiation data (8). The total doses used were: 26.1 and 34.2 Gy (3F) ; 30.8 and 40.4 Gy (6F) ; 34.0 and 44.5 Gy (9F). Seven months after irradiation bone blood flow changes were measured by fractional distribution of ^{86}RbCl (83) and the red blood cell volume by the dilution of ^{51}Cr labelled red cells. The injection and measuring techniques were the same as that with the ^{125}I antipyrine extraction technique. The bone mineral content was estimated by measuring the dry bone weight.

In reference (10) the bone marrow in the left femur was irradiated with single doses of 5,10,15,20 and 25 Gy. One, three and seven months postirradiation changes in bone marrow blood flow were measured by fractional distribution of ^{125}I antipyrine (83). Fractionated irradiations of the bone marrow were given in 3,6 and 9 fractions during 3 weeks. The total doses were 26.1 and 34.2 Gy (3F) ; 30.8 and 40.4 Gy (6F) ; 34.0 and 44.5 Gy (9F). The changes in bone marrow blood flow were measured by ^{86}RbCl 7 months postirradiation. The RBC volume was measured by ^{51}Cr labelled red cells.

In reference (11) the patients received fractionated ^{60}Co

radiation therapy with the four beam box technique for different carcinomas of the pelvic area, where the lateral fields intersected the proximal parts of the femurs. Blood flow in the bone was measured bilaterally from the trochanteric areas of the femurs using a ^{133}Xe wash-out method (92), where the wash-out curves were analyzed using a two-compartmental exponential model. The bone blood flow was calculated from equation: $F=w_1(m)f_1+w_2(m)f_2$,where $w_1(m)$ and $w_2(m)$ are the fractional weights of the components of the two-exponential curve: $C(t)=A_1e^{-k_1t} + A_2e^{-k_2t}$. The parameters k_1 and k_2 are the flow/volume ratios of the components. The fractional weights are calculated from a formula : $w_i=(A_i/f_i)/(A_1/f_1+A_2/f_2)$, where f_1 represents the blood perfusion in hematopoietic tissue of bone marrow and f_2 blood perfusion in non-hematopoietic tissue of bone. The absorbed dose in the volume of the ^{133}Xe bone blood flow measurement was estimated from the dose plan of each patient. The total absorbed dose to bone in the measuring area varied from 19.0 to 30.0 Gy for different patients. The estimated maximum variation in the dose across the volume of blood flow measurement was under 10 per cent. The total treatment time varied from 7 to 10 weeks.

In reference (12) the brains of the rats were irradiated bilaterally with two parallel opposed fields. In single dose experiments 11.9, 14.5, 17.0, 19.6 and 22.1 Gy was given. In fractionated treatments 4,7 or 10 fractions were given over a fixed time of 3 weeks. The fractionated doses (FD) were calculated according to the formula: FD = single dose x $N^{0.42}$, where N = number of fractions. Thus the total doses for the

different fractionation schemes were : 4F: 21.3, 25.8, 30.4, 35.0 and 39.5 Gy ; 7F: 27.0, 32.7, 38.5, 44.3 and 50.1 Gy ; 10F: 31.3, 38.0, 44.7, 51.4 and 58.1 Gy. Radiation induced brain blood flow changes were measured 9 months after irradiation using an ^{125}I antipyrine extraction technique (83), where a bolus of ^{125}I antipyrine was injected into a femoral vein. After an interval of 15 seconds the animals were sacrified by decapitation. The skull was then rapidly opened and the whole brain dissected out. The radioactivity in the samples was measured in a well-type NaI counter. A standard dilution was made to get the extraction ratio in terms of the percentage of the injected dose of ^{125}I antipyrine/g of brain tissue.

8.0 RESULTS

(8) In 12 month old rats 0.14 % of the ^{125}I antipyrine injected was extracted by the normal nonirradiated femur. The changes in the relative extraction of ^{125}I antipyrine in femoral bone were time and dose dependent. The largest decrease in antipyrine extraction was found after an interval of 3 months, the difference being nearly significant ($p<0.05$) at all the dose levels. In femurs irradiated with 5 to 20 Gy, antipyrine extraction was not significantly different from that in the contralateral limb 7 months after irradiation, but it still was reduced in those receiving 25 Gy. The dry weight of irradiated bone was about same as in the contralateral side at one and 3 months after irradiation. After 7 months nearly significant ($p<0.05$) changes were found after single doses of 15,20 and 25 Gy.

Seven months after 25 Gy irradiation the calcium/phosphorous ratio was similar in irradiated and control bones.

(9) In the irradiated femoral bone the reduction of $^{86}RbCl$ extraction was statistically significant for all fractionation schemes used. There was no significant difference between the fractionation schemes at each NSD level. However, the effect was greater for the higher

NSD value. The RBC volume was similar in the irradiated side compared to that in the control femur on all the dose levels used. The bone weight was reduced from 3 to 6 %. The reduction was slightly higher on the higher NSD level.

(10) Single dose irradiations:

One month after irradiation the reduction of ^{125}I antipyrine extraction in bone marrow was slight, being statistically significant only after doses of 20 and 25 Gy. After a latent period of 3 months the reduction was greater. In bone marrow irradiated with 15 Gy the antipyrine extraction had increased by approximately 25 % 7 months after irradiation. With doses of 20 and 25 Gy the extraction remained at about the same reduced level as seen after 3 months.

Fractionated irradiations:

The reduction in both $^{86}RbCl$ extraction and the RBC volume in bone marrow was statistically significant in all fractionation schemes. In the fractionation schemes of 3 F and 6 F the $^{86}RbCl$ extraction was significantly lower with the NSD of 1900 ret compared to that for 1450 ret.

The reduction of RBC volume was slightly greater after 1900 ret compared to that with 1450 ret. However, the reduction in RBC volume was from 23 to 37 % greater in the 3 F groups compared to that in the 9 F groups.

(11) Bone blood flow was slightly decreased during the first half of the treatment course. At the end of radiotherapy, bone blood flow returned about to the preirradiated level. Some patients had a marked reduction of blood flow from two to 18 months after radiotherapy.

(12) In the age-matched control group of rats the brain tissue extracted 0.93 % (0.04 % 1SE) of the injected dose of ^{125}I antipyrine per g of brain tissue. The extraction of ^{125}I antipyrine in the irradiated rats varied from 0.91 to 1.36 %, being on the average 20.4 % higher than that in the control group.

There was no significant difference in the antipyrine extraction between different fractionation schemes.

The value of the exponent of N in all the modified Ellis' formulas for CNS tolerance that are available in the literature varied from 0.33 to 0.56, the mean value being 0.42 (0.05 1SE).

9.0 DISCUSSION

The extraction methods used to estimate the blood flow are based on the principle that the initial fractional uptake of tracer is equal to the blood flow fraction of the cardiac output (83). The animal studies were started with ^{125}I antipyrine extraction technique. Because ^{125}I antipyrine was no longer available $^{86}RbCl$ was used, as well. Both tracers are freely diffusible. In most tissues an equilibrium was reached within the intracellular space after 10-20 seconds (93). The equilibrium state, lasting for at least five minutes, is the measure of regional vascular perfusion (73). However, the uptake of $^{86}RbCl$ in brain tissue is very low. Probably the blood-brain barrier prevents the exchange of the potassium analog ^{86}Rb (83). Iodo-antipyrine is lipid soluble and crosses the blood-brain barrier. The extraction of iodo-antipyrine in the CNS is similar to that in other normal tissues (93).

In the present experiment no absolute values of blood flow were derived. Therefore, the differences in partition coefficient of tracers between different tissues (bone, bone marrow, brain tissue) were not taken into consideration. However, the present investigation does assume the partition coefficient of the tracer to be the same for both normal and irradiated tissue. Sapirstein (83) has assumed that the extraction both of $^{86}RbCl$ (except in CNS) and of iodo-antipyrine is flow limited. However, the changes in extraction do not take into account any modification in the surface area of the capillary walls, which may be available to a tracer for exchange. Thus the surface-permeability-product may

alter due to the change in surface area.

The radiation induced changes in bone and bone marrow blood flow were time related. The timing of the maximum reduction in the blood flow, 3 months after irradiation, was comparable with changes seen in the skin (94), lung (73,95), hamster cheek pouch (96) and bone marrow (97).

At seven months after irradiation the blood flow in the femoral bone was improved after 25 Gy and returned to normal level after 15 and 20 Gy. However, the reduction in the weight of the irradiated bone was present. Therefore, reduced blood flow 3 months after irradiation would seem to be an important factor in the subsequent atrophy of bones.

In bone marrow, an approximate 25 % improvement in blood flow was observed between 3 and 7 months after a dose of 15 Gy. With 20 or 25 Gy the improvement of the blood flow was minimal. Knospe et al.(98) observed diffuse hemopoietic regeneration 6-12 months after a dose of 20 Gy. They noted that the maximum reduction in marrow cellularity, seen after two to three months, correlated well with the disappearance of the marrow sinusoidal architecture.

The dose levels used in fractionated bone and bone marrow studies were based on the results from the previous studies where single doses were used. To study late changes in bone marrow the measurements were done 7 months after irradiations. However, according to the single dose experiments the reduction of tracer

extraction was maximal at 3 months and an improvement was seen from 3 to 7 months. This reduces the sensitivity of the extraction as the parameter for radiation induced damage at 7 months.

The effect of different dose fractionation schedules on bone tissue was unknown. Therefore, the predictive value of the NSD formula for the tolerance of hard bone was tested. The parameters of the LQ model have been derived (6) for early reactions in bone marrow after whole body irradiation. But the effects of fractionated irradiation for both local irradiation and for late reactions were not known.

Due to the sensitivity of the assay methods used, it was not possible to evaluate the isoeffect curve for radiation tolerance of hard bone in relation to the number of fractions. However, the dose levels predicted by the NSD formula produced approximately the same damage to the rat femur seven months postirradiation. The results for the fractionated irradiation in bone marrow would suggest a value of the α/β ratio of between 2 and 4 Gy. This corresponds very well to the values presented for other normal tissues (54). For late reactions the ratio in most tissues is under 4 Gy.

The study of human bone blood flow with a small number of patients suggests for the first time that a decrease of blood flow with fractionated doses below 30 Gy shortly after irradiation is small. However, there is a significant decrease in blood flow (about 50 %) several months after the radiotherapy.

More measurements in a later phase of recovery are needed to find the late radiation tolerance of human bone after fractionated radiotherapy.

In testing the fractionation model for brain tissue a dose response for the extraction of ^{125}I antipyrine was measured after single and fractionated doses of X-rays. The model used was: fractionated dose= single dose x $N^{0.42}$. The value of 0.42 in the exponent of N corresponds to the average value reported in literature for the central nervous system (Table I). The time factor effect was excluded from our model because its contribution would be minimal for late effects in CNS (see Table I). The ^{125}I antipyrine extraction was measured 9 months after irradiation when the dose related changes in the extraction were highest (99). In the irradiated rats the ^{125}I antipyrine extraction was on average 20.4 % higher than that in the control group. The increase of the extraction may be due to an increase in the surface area of blood vessels available to the tracer. Both morphological studies and radiotracer techniques indicate an increase in blood volume from 6-18 months after a single dose of 20-25 Gy (100).

In the single dose, four fraction and ten fraction groups, the extraction was approximately at the same level. The exponent 0.42 corresponds to the α/β ratio of about 2.0 Gy in the LQ model. Only a very limited amount of data was available for brain tissue. The α/β ratios for rat and human brain tissue of 6.0 (6) and 4.2 Gy (35), respectively, have been reported. The present study showed that the NSD formula highly underestimates the late radiation damage in brain tissue when a small number of large fractions are used.

10.0 APPENDIX: SYMBOLS AND ABBREVIATIONS:

D_0 mean lethal dose (Gy)

D absorbed dose (Gy)

CMT composite multi-target

LQ linear quadratic

RMR repair-misrepair

NSD nominal standard dose

D_{tol} tolerance dose (Gy)

N number of fractions in the whole treatment course

T over-all treatment time (days)

n number of fractions ($n \leqq N$)

t over-all period of t days ($t \leqq T$)

PT partial tolerance

TDF time, dose and fractionation

d dose per fraction (Gy)

CRE cumulative radiation effect

DF decay factor

R duration of rest period (days)

T_0 time (one day)

S_J surviving fraction

n_t number of targets

S_K surviving fraction

S total survival

K radiosensitivity constant for cumulative sublethal effects in CMT model(1/Gy)

J initial slope of the survival curve in CMT model (1/Gy)

S_N survival after N equal treatments

α initial slope of the survival curve in the LQ model (1/Gy)

β radiosensitivity constant for cumulative sublethal effects in the LQ model ($1/Gy^2$)

D_t total dose (Gy)

L lethality

M mutation

U uncommitted lesion

R_s repair state

R_l linear repair process

R_q quadratic repair process

c_l coefficient of linear repair

c_q coefficient of quadratic repair

R_r repair ratio (cl/cq)

a yield of U lesions per rad

β_e effective mass attenuation coefficient of the electrons (m^2/kg)

X exposure (C/kg)

Q charge (C)

W mean energy required to produce an ion pair (J)

m mass (kg)

e charge of a electron (C)

μ_{en} energy absorption coefficient (1/m)

ρ density (kg/m^3)

μ_{en}/ρ mass energy absorption coefficient (m^2/kg)

μ_{tr} energy transfer coefficient (1/m)

μ_{tr}/ρ mass energy transfer coefficient (m^2/kg)

K_{air} air kerma (Gy)

g fraction of the energy of secondary charged particles that is lost to bremstrahlung

S stopping power (J/m)

S/ρ mass stopping power (Jm^2/kg)

s_{maga} mass stopping power ratio (material/gas)(Jm^2/kg)

I_{ma} equilibrium electron spectrum in the medium

E energy(J)

Z atomic number

A atomic weight

B stopping number

d_w a weighting factor in Burlin cavity theory

g_p average path lenght of electrons (m)

11.0 REFERENCES

(1) H.R. Withers, L.J. Peters and H.D. Kogelnik, Radiation Biology in Cancer Research, eds. R.E. Meyn and H.R. Withers (Raven Press, New York 1980) pp. 439-448

(2) D.T. Goodhead, Radiation Biology in Cancer Research, eds. R.E. Meyn and H.R. Withers (Raven Press, New York 1980) pp. 231-247

(3) W.E. Liversage, Br. J. Radiol. 42 (1969) 432

(4) J. Kirk, W.M. Gray and E.R. Watson, Clin. Radiol. 23 (1972) 93

(5) J. Kirk, W.M. Gray and E.R. Watson, Clin. Radiol. 24 (1972) 1

(6) G.W. Barendsen, Int. J. Radiat. Oncol. Biol. Phys. 8 (1982) 1981

(7) L. Cohen, Cancer 32 (1973) 236

(8) M.A. Pitkänen and J.W. Hopewell, Acta Radiol. Oncol. 22 (1983) 253

(9) M.A. Pitkänen and T. Hietanen, Strahlentherapie 160 (1984) 394

(10) M.A. Pitkänen and J.W. Hopewell, Strahlentherapie (in press)

(11) T. Lahtinen, M.A. Pitkänen and A. Ojala, Strahlentherapie (submitted for publication)

(12) M.A. Pitkänen and J.W. Hopewell, Acta Radiol. Oncol. (in press)

(13) M. Strandqvist, Acta Radiol. Oncol. suppl.55 (1944) 1

(14) F. Ellis, Clin. Radiol. 20 (1969) 1

(15) J. Kirk, W.M. Gray and E.R. Watson, Clin. Radiol. 22 (1971) 145

(16) C.G. Orton and F. Ellis, Br. J. Radiol. 46 (1973) 529

(17) B.M. Winston, F. Ellis and E.J. Hall, Clin. Radiol. 20 (1969) 8

(18) E.D. Montague, Radiology 90 (1968) 962

(19) W.E. Liversage, Br. J. Radiol. 44 (1971) 91

(20) J.C. Horiot, G.H. Fletcher, A.J. Ballantyne and R.D. Lindberg, Radiology 103 (1972) 663

(21) G. Arcangeli, M. Friedman and R. Paolugi, Br. J. Radiol. 47 (1974) 44

(22) T.D. Bates and L.J. Peters, Br. J. Radiol. 48 (1975) 773

(23) R.W. Byhardt, M. Greenberg and J.D. Cox, Int. J. Radiat. Oncol. Biol. Phys. 2 (1977) 415

(24) K. Singh, Br. J. Radiol. 51 (1978) 357

(25) H.R. Withers, H.D. Thames and B.L. Flow Jr., Int. J. Radiat. Oncol. Biol. Phys. 4 (1978) 595

(26) W.J. Spanos, E.D. Montague and G.H. Fletcher, Int. J. Radiat. Oncol. Biol. Phys. 6 (1980) 1473

(27) W.T. Sauce, J.R. Steward, H.P. Plenk and D.D. Levitt, Int. J. Radiat. Oncol. Biol. Phys. 7 (1981) 1541

(28) S. Dische, W.M.C. Martin and P. Andersen, Br. J. Radiol. 54 (1981) 29

(29) R.H. Fitzgerald, R.D. Marks and K.M. Wallace, Radiology 144 (1982) 609

(30) H.D. Thames, H.R. Withers, L.J. Peters and G.H. Fletcher, Int. J. Radiat. Oncol. Biol. Phys. 8 (1982) 219

(31) I. Turesson and G. Notter, Int. J. Radiat. Oncol. Biol. Phys. 10 (1984) 593

(32) I. Turesson and G. Notter, Int. J. Radiat. Oncol. Biol. Phys. 10 (1984) 599

(33) F. Ellis, Br. J. Radiol. 53 (1980) 821

(34) L. Cohen and M. Creditor, Int. J. Radiat. Oncol. Biol. Phys. 7 (1981) 961

(35) L. Cohen and M. Greditor, Int. J. Radiat. Oncol. Biol. Phys. 9 (1983) 233

(36) W.M. Wara, T.L. Phillips, G.E. Sheline and J.G. Schwade, Cancer 35 (1975) 1558

(37) A.J. Kogel van der, Radiology 122 (1977) 505

(38) K. Masuda, B.O. Reid and H.R. Withers, Radiology 122 (1977) 239

(39) A. White and S. Hornsey, Br. J. Radiol. 51 (1978) 515

(40) S. Hornsey, C.C. Morris and R. Myers, Int. J. Radiat. Oncol. Biol. Phys. 7 (1981) 393

(41) R.D. Pezner and J.O. Archambean, Int. J. Radiat. Oncol. Biol. Phys. 7 (1981) 397

(42) D.R. Wigg, K. Koschel and G.S. Hodgson, Br. J. Radiol. 54 (1981) 787

(43) T.T. Puck and P.I. Marcus, J. Exptl. Med. 103 (1956) 653

(44) M.A. Bender and P.C. Cooch, Int. J. Radiat. Biol. 5 (1962) 133

(45) E.H. Porter, Br. J. Radiol. 38 (1964) 607

(46) L. Cohen, Br. J. Radiol. 41 (1968) 522

(47) L. Cohen and J.E. Moulder, Radiat. Res. 76 (1978) 250

(48) L. Cohen and M. Creditor, Int. J. Radiat. Oncol. Biol. Phys. 9 (1983) 1065

(49) R. Wideröe, Acta Radiol. Oncol. 4 (1966) 257

(50) R. Wideröe, Strahlentherapie 148 (1974) 46

(51) E. Spring and K. Paasikallio, Strahlentherapie 140 (1970) 503

(52) A.M. Kellerer and H.H. Rossi, Radiat. Res. 47 (1971) 15

(53) S. Hornsey and A. White, Br. J. Radiol. 53 (1980) 168

(54) J.F. Fowler, Br. J. Radiol. 56 (1983) 497

(55) J.F. Fowler, Br. J. Cancer 49 (1984) 285

(56) A.J. Kogel van der, Cytotoxic Insult to Tissues, eds. C.S. Potten and J.H. Hendry (Churchill-Livingstone, Edinburgh 1982) pp. 329-352

(57) J.T. Leith, J.K. de Wyngaert and A.S. Glicksman, Int. J. Radiat. Oncol. Biol. Phys. 7 (1981) 1673

(58) C.A. Tobias, E.A. Blakely, F.Q. Ngo and T.C.H. Yang, Radiation Biology in Cancer Research, eds. R.E. Meyn and H.R. Withers (Raven Press, New York 1980) pp. 195-230

(59) ICRU Report 33, International Commision on Radiation Units and Measurements, Washington 1980

(60) W.H. Gray, Studies in Radioactivity, Macmillan, New York 1912

(61) L.H. Gray, Proc. Roy. Soc. A156 (1936) 578

(62) L.V. Spencer and F.H. Attix, Radiat. Res. 3 (1955) 239

(63) T.E. Burlin, Br. J. Radiol. 39 (1966) 727

(64) Y.S. Horowitz and A. Dubi, Phys. Med. Biol. 27 (1982) 867

(65) A. Janssens, Phys. Med. Biol. 28 (1983) 745

(66) A. Shiragai, Phys. Med. Biol. 29 (1984) 427

(67) K. Shimanovskaya and A.D. Shiman, Radiation Injury of Bone, Pergamon Press, New York 1983

(68) ICRU Report 37, International Commission on Radiation Units and Measurements, Washington 1984

(69) F.W. Spiers, Br. J. Radiol. 22 (1949) 521

(70) F. Ellis, Br. J. Radiol. 32 (1959) 588

(71) J.W. Hopewell and E.A. Wright, Br. J. Radiol. 43 (1970) 161

(72) L.F. Fajardo and J.R. Stewart, Radiology 101 (1971) 429

(73) E. Glatstein, Radiat. Res. 53 (1973) 88

(74) H.S. Reinhold, Curr. Top. Radiat. Res. Q. 10 (1974) 58

(75) J.W. Hopewell, J.L. Foster, C.M.A. Young and G. Wiernik, Radiology 130 (1979) 783

(76) D.W. Hebard, K.L. Jackson and G.M. Christensen, Radiat. Res. 81 (1980) 441

(77) D.G. Hirst, J. Denekamp and E.L. Travis, Radiat. Res. 77 (1979) 259

(78) J.W. Hopewell, Radiation Biology in Cancer Research, eds. R.E. Meyn and H.R. Withers (Raven Press, New York 1980) pp. 449-459

(79) J.R. Maisin, Curr. Top. Radiat. Res. Q. 10 (1974) 29

(80) J.W. Hopewell, Br. J. Radiol. 47 (1974) 157

(81) T.S. Phillips, Radiology 87 (1966) 49

(82) H.S. Reinhold, Curr. Top. Radiat. Res. Q. 10 (1974) 9

(83) L.A. Sapirstein, Am. J. Physiol. 193 (1958) 161

(84) R. Studer and E.J. Potchen, J. Nucl. Med. 10 (1969) 442

(85) M.M. Graham, Radiat. Res. 51 (1972) 519

(86) P. Rubin and G.W. Casarett, Clinical Radiation Pathology, Saunders, Philadelphia 1968

(87) H.S. Reinhold and G.H. Buisman, Br. J. Radiol. 46 (1973) 54

(88) J.W. Hopewell and T.J.S. Patterson, Biorheology 9 (1972) 46

(89) D.G. Hirst, J. Denekamp and B. Hobson, Cell and Tissue Kinetics 13 (1980) 91

(90) J.W. Hopewell, Cytotoxic Insult to Tissues, eds. C.S. Potten and J.H. Hendry (Churchill-Livingstone, Edinburgh 1982) pp. 228-257

(91) P.S. Chen, Analyt. Chem. 28 (1956) 1756

(92) T. Lahtinen, P. Karjalainen and E.M. Alhava, Eur. J. Nucl. Med. 4 (1979) 435

(93) L.A. Sapirstein and G.E. Hanusek, Am. J. Physiol. 193 (1958) 272

(94) J.W. Hopewell, J.L. Foster, Y. Gunn, H.F. Moustafa, T.J.S. Patterson, G. Wiernik and C.M.A. Young, Late Biological Effects of Ionising Radiation, vol 1. (IAEA; Vienna 1978) pp.483-492

(95) H.F. Moustafa and J.W. Hopewell, Radiobiological Research and Radiotherapy, vol 1. (IAEA, Vienna 1977) pp.75-83

(96) J.W. Hopewell, Radiat. Res. 63 (1975) 157

(97) M.A. Maloney and H.M. Patt, Radiat. Res. 50 (1972) 284

(98) W.H. Knospe, J. Blom and W.H. Crosby, Blood 28 (1966) 398

(99) H.F. Moustafa and J.W. Hopewell, Br. J. Radiol. 53 (1980) 21

(100) H.S. Reinhold and J.W. Hopewell, Br. J. Radiol. 53 (1980) 693